Prediction the durability of heat exchangers made of 06KhN28MDT alloy (analogous to AISI904L steel) to crevice corrosion during their operation in recycled water

A.V. Dzhus* and G.V. Snizhnoi

Zaporizhzhia Polytechnic National University, Zaporizhzhia, Ukraine
*e-mail: dzhus_anna@zp.edu.ua

Plate-like heat exchangers commonly use 06KhN28MDT alloy for various acids, which is resistant to localized corrosion but susceptible to crevice corrosion in cooling water. This study assessed the alloy's crevice corrosion resistance in 3% NaCl circulating water using electrochemical methods. Anodic potentiodynamic curves determined Er, Ecor, and Ecrew potentials. Resistance was assessed based on Ecrew potential, simulating a 0.3 mm gap. Ecrew potentials varied: melts 1 and 5 were most positive (1.10 and 1.13V), melts 2 and 3 the most negative (0.58V), due to differences in Cr, Mo, Ti, Cu content. Melts 2 and 3, with excess carbon, had negative Ecrew potentials. No correlation was found between Ecrew and titanium nitride volume, but melt 1 had more than melts 2 and 5. ΔE, the difference between Er and Ecor, produced similar results. Melts 1, 4, and 5 were highly resistant, melts 2 and 3 less so. In conclusion, heat exchanger manufacturers should choose low-C, high-Cr, Mo, Ti, Cu alloy for better crevice corrosion resistance in circulating water.

Key words: crevice corrosion, plate-like heat exchanger, model circulating water, chloride-containing media.
PACS number(s): 81.40.Np.

1 Introduction

The 06KhN28MDT alloy (similar to AISI904L stainless steel) is used in the production of plate-like heat exchangers, which are used in the production of sulfuric, orthophosphoric, hydrofluoric acid, etc. [1]. After all, they have high corrosion resistance to intercrystalline corrosion in these media [2]. But the circulating water, which is used to cool the technological product during the production of acids, contains chlorides and other anions [3-6], which can be the cause of pitting or crevice corrosion of heat exchangers [7-10]. In particular, design features of plate-like heat exchangers and chlorides in circulating water can be the cause of their crevice corrosion between the corrugations of adjacent plates. Today, there are many studies devoted to the assessment and prediction of pitting resistance of steels AISI304 [8], AISI321 [12, 13] and alloy 06KhN28MDT [7-10], which are used in the production of plate-like heat exchangers. In papers [10-12], the patterns and mechanisms of the genesis and growth of pitting on their surface in chloride-containing media have been investigated, in paper [13] a method for identifying stable and metastable pitting has been proposed, and in [11,12] it has been established that the critical pitting temperatures of the above-mentioned structural materials mainly depend on their structural heterogeneity and the parameters of the chloride-containing media. Crevice and pitting corrosion of steels and alloys have many common features [15], in particular, pitting corrosion of heat exchanger plates under sediment from circulating water on their surface can turn into crevice corrosion when the chloride-containing media in the gap between them is acidified or alkalized with a simultaneous increase in chloride content [3]. Under such conditions, pitting on the surface of the heat exchange plates from the circulating water side grows intensively and turns into corrosion ulcers. At the same time, the intensity of their growth no longer depends on the parameters of the chloride-containing media (pH, chloride concentration). Therefore, the article investigated the influence of the parameters of the 06KHN28MDT alloy on its resistance to crevice corrosion in circulating water during the operation of plate-like heat exchangers.

2 Research materials and methods of investigation

Five industrial melts of the 06KhN28MDT alloy have been studied. Their chemical composition and structural heterogeneity have been determined earlier [10]. The specific magnetic susceptibility of the alloy has been determined in [16]. Electrochemical tests of the alloy have been carried out on samples of 1 mm thick sheets cut along the rolled length. Polished samples 30×20×1mm with a hole ø 6mm have been assemed in block. The gap between the sample and the counterface, which are made of the same material (Table 1), has been fixed with fluoroplastic washers. The gap between the sample and the counterface was 0.3 mm, which corresponds to the gap between adjacent plates of the plate-like heat exchanger.

Electrochemical studies have been carried out on the P5848 potentiostat. Before the start of polarization, the samples were kept in a 3% NaCl solution for 10 minutes until the E_{cor} free corrosion potential has been established and anodically polarized at a rate of 1.8 V/hour. Potentiodynamic anodic curves of direct move have been recorded up to a current density of 30 mA/cm². The mistake of determining the potentials of E_{crew} crevice corrosion and E_r repassivation in the crevice did not exceed ±0.01V.

Table 1 – Chemical composition of alloy 06KHN28MDT (similar to AISI904L steel)

Melting number	The content of alloying elements, wt. %									
	C	Si	Mn	Cr	Ni	Mo	Cu	Ti	S	P
1	0.050	0.60	0.32	24,31	27,39	2.90	2.75	0.79	0.006	0.029
2	0.067	0.57	0.46	22.68	27.65	2.78	2.68	0.59	0.005	0.027
3	0.068	0.55	0.54	21.84	27.45	2.55	2.60	0.55	0.004	0.038
4	0.048	0.62	0.57	22.67	27.73	2.56	2.53	0.67	0.006	0.028
5	0.050	0.57	0.31	23.46	27.51	2.51	2.78	0.89	0.004	0.032

3 Results and their discussion

The analysis of the constructed anodic potentiodynamic curves of the 06KHN28MDT alloy showed that the forward and reverse move curves of all five melts crossed several times (Fig. 1). This may indicate that during anodic polarization of the alloy on the surface of the samples and the counterface, pitting has been generated and repasivated. The pittings were most repasivated in the melts 1, 5 of the 06KHN28MDT alloy (Fig. 1, a), since in them the anode potentiodynamic curves of forward and reverse move most often crossed before the formation of a hysteresis loop (Fig. 1). It is obvious that this is caused by the highest content of Cr, Mo and Cu in the melt No. 1 and Cr and Cu in No. 5 (Table 1). It is known [17] that Cr and Mo contribute to the repassivation of pitting in chloride-containing media. In addition, the effect of alloying elements Cr, Mo and Cu on the electrochemical behavior of steel depends on the potential. In particular, in the active area, in conditions, when the corrosion rate is determined by the anodic dissolution of the main elements, Mo and Cu contribute to the formation of a passive film enriched in Cr [18]. It is considered [19, 20] that Mo increases the resistance of passive films to "breakdown" in chloride-containing media, increases passivation characteristics [21] and reduces the rate of metal dissolution in pitting [22]. In the paper [23], they found that Mo together with Cr form mixed oxides in the passive film, which are more corrosion-resistant than chromium oxides. This hypothesis is based on the fact that Mo increases the pitting resistance of chromium-nickel steels in chloride-containing media, while iron-molybdenum alloys not alloyed with Cr and Ni are prone to pitting [24]. The authors of the work [25] believe that the improvement of the protective properties of passive films in neutral solutions as a result of additional alloying of Mo steels is due to the adsorption of MoO_4^{-2} ions on them, formed as a result of oxidative dissolution of Mo from them and poushing out of chloride ions from their surface [23, 24]. But we consider that, most likely, the aforementioned corrosion behavior of melts 1, 5 of the 06KhN28MDT alloy (Fig. 1 a) is associated with the formation of mixed Cr, Mo oxide films on its surface. The role of Cr in the protective properties of these films is more important than that of Mo, since the E_r of No. 1 is more positive than that of No. 5 (table 2), and the content of Mo in No. 1 is maximum (2.88 wt. %), and in No. 5 it is minimum (2.53 wt. %) (Table 1). In addition,

works [8-10] established that the pitting resistance of stainless steels AISI304, AISI321, 12Kh18N10T, 08Kh18N10 and the alloy 06KhN28MDT depends, first of all, on the parameters of the chloride-containing media (pH, chloride concentration), their structural heterogeneity and increases only with an increase in their chromium content within the standard. But in the melts 1, 5 of the 06KhN28MDT alloy was found to have the highest content of Cr and Cu, and No. 1 also contained Mo (Table 1). This contributed to establishing the most positive value of the repassivation potential (0.8 V) in melt 1, since it is known [15] that Mo and Cu contribute to the formation of a passive film enriched in Cr. It has been established that the areas of the hysteresis loop of the melts of the investigated alloy increase in the following order: melts 3, 2, 4, 5, 1 (Fig. 1). This is due to the fact that there is less in the Cr and Cu alloy (Table 1), the area of the hysteresis loop is also smaller, but there is more corrosion damage on the samples after their examination in model circulating water.

Table 2 – Indicators of alloy 06KhN28MDT

Melting number	χ_0, 10^{-8} m³/kg	E_{cor}, V	E_{crev}, V	E_r, V	ΔE, V	d_g, μm
1	2.95	-0.40	1.10	0.80	1.20	50
2	2.86	-0.43	0.58	0.50	0.93	67
3	3.38	-0.42	0.58	0.22	0.64	68
4	3.09	-0.40	1.10	0.55	0.95	48
5	2.96	-0.38	1.13	0.60	0.98	50

It has been established that the area of the hysteresis loop of the studied alloy (Fig. 1) correlates with the potentials E_{crew} and E_r, which were established in the gap between the sample and the counterface (Table 2), they also shift in the positive direction in the following order: melts 3, 2, 4, 5, 1. It has been found that the more positive the value of the E_{crew} and E_r potentials of the alloy, the larger the area of corrosion damage on its surface. But the larger it is, the higher the ΔE value of the alloy in the crevice, which determines its resistance to crevice corrosion (Table 2).
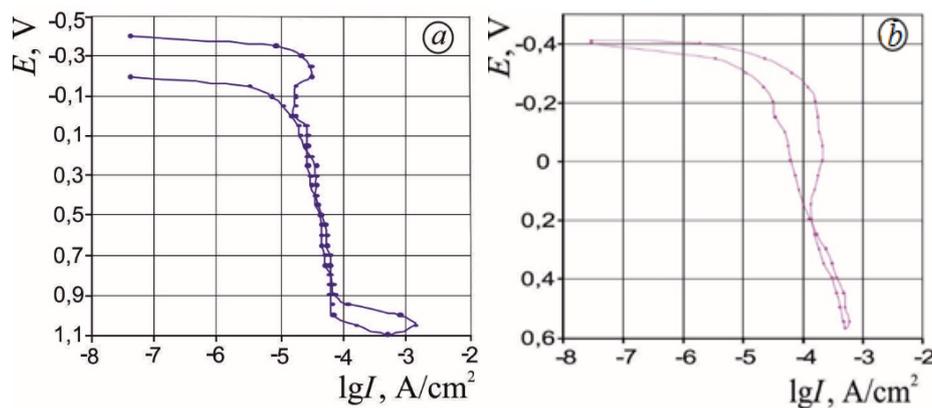

Figure 1 – Anodic potentiodynamic curves of forward and reverse move
of 06KhN28MDT alloy: a) melt 1, b) melt 3

This is most likely due to the fact that the more local corrosion centers on the surface of the alloy, the lower the intensity of their growth. This is consistent with the data of the work [15]. According to the results of the analysis (Fig. 2 b), it has been established that in the model circulating water, the E_{crew} potential of

the 06KhN28MDT alloy intensively shifts to a more negative direction from 1.13 melt 5 to 0.58 V melts 2, 3 with an increase in the C content in it from 0.05 melt 5 to 0.067; 0.068 wt. % melts 2, 3. This is most likely due to the fact that at such a concentration of C in the alloy, carbides may precipitate from a solid solution of austenite, since the maximum solubility of C in it is about 0.05 wt. % [26-28].
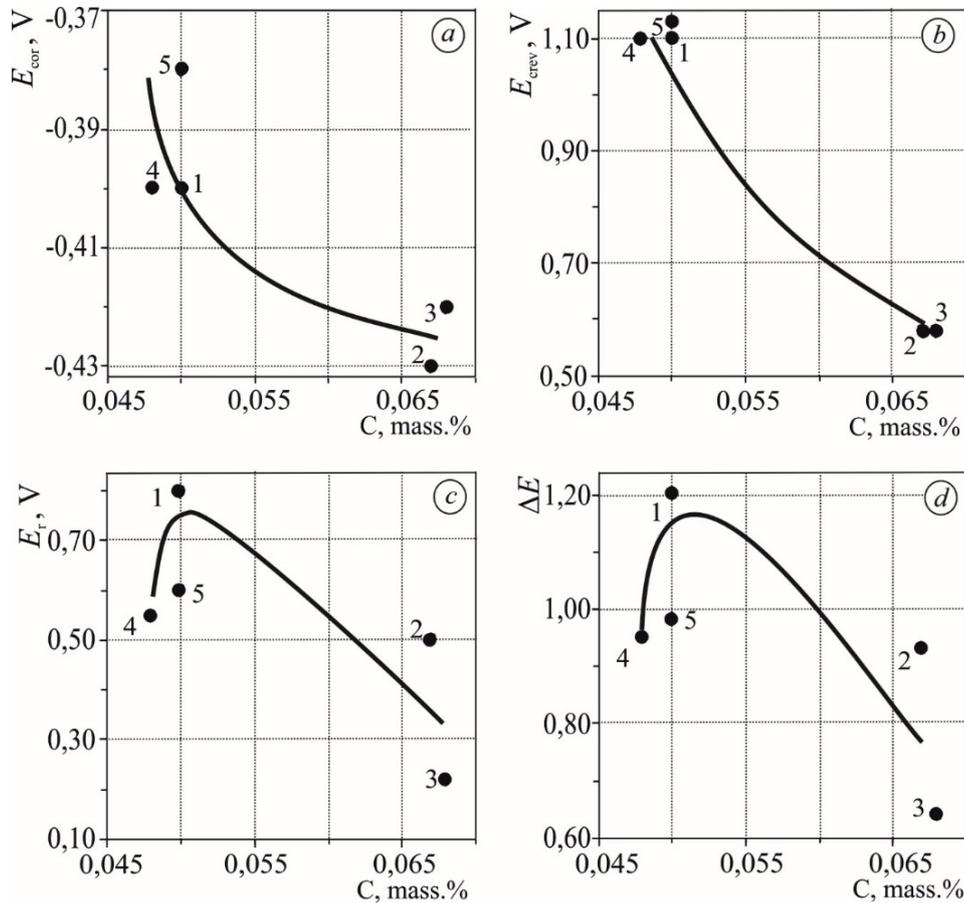
Figure 2 – Dependence of potentials E_{cor} (a), E_{crew} (b) and E_r (c) and crevice corrosion resistance basis ΔE (d) of the 06KhN28MDT alloy on its carbon content

According to the results of the analysis (Fig. 2, a), it has been established that the potential of free corrosion (E_{cor}) of the 06KhN28MDT alloy slowly shifts to a more negative direction from -0.38 (melt 5) to -0.43 (melt 2) with an increase in its carbon content from 0.05 (melt 5) to 0.067 wt.% (melt 2) (table 2). It can be assumed that the mechanisms of influence of C in the alloy on the potentials of E_{cor} and E_{crew} are the same, since similar dependencies have been established between them and the carbon content (Fig. 2 a, b). It has been established that the repassivation potential E_r of the alloy in the gap depends ambiguously on the content of carbon in it (Fig. 2 c). In particular, it rapidly shifts in the more positive direction from 0.55 (melt 4) and 0.60 (melt 5) to 0.80 V (melt 1) with an increase in its carbon

content from 0.048 (melt 4), 0.05 (melt 5) to 0.05 wt. % (melt 1). It turns out that the maximum saturation of the solid solution of the austenite alloy with carbon within the limits of its solubility contributes to the shift of the E_r potential in a more positive direction. Perhaps this is due to the influence of C on the specific magnetic susceptibility of austenite (χ_0) of the alloy, since it has been established that it also rapidly shifts in the more positive direction from 0.5 (melt 2) to 0.8 V (melt 1) with an increase in the parameter (χ_0) from $2.86 \cdot 10^{-8}$ (melt 2) to $2.95 \cdot 10^{-8}$ m³/kg (melt 1) (Fig. 3c). It should be noted that the E_r potential of the 06KhN28MDT alloy shifts to a more negative direction from 0.8 (melt 1) to 0.22 V (melt 3) with an increase in its carbon content from 0.05 (melt 1) to 0.068 wt. % (melt 3) (Fig. 2 c). This, as mentioned

above, may be due to precipitation of carbides (Cr, Mo, Ti) from the austenite solid solution. At the same time, it should be noted that the shift of the E_r potential to the negative side with increasing carbon content in the alloy in this interval is due not only to the precipitation of carbides from the austenite solid solution, but also to a decrease in the χ_0 parameter in it (see Fig. 2c and Fig. 3c).

Similar relationships (Fig. 2 c, d) between the E_r potential of the 06KhN28MDT alloy, the basis of its resistance to crevice corrosion (ΔE) and its C content have been established. Therefore, taking into account the established dependence of E_{cor} (C) (Fig. 2a), it can be noted that the resistance of the 06KhN28MDT alloy to crevice corrosion in model circulating water mainly depends on the E_r potential, since the ΔE criterion of the alloy in the crevice is determined by the difference between the E_r and E_{cor} potentials [29] In addition, the larger it is, the higher the resistance of the alloy to crevice corrosion.
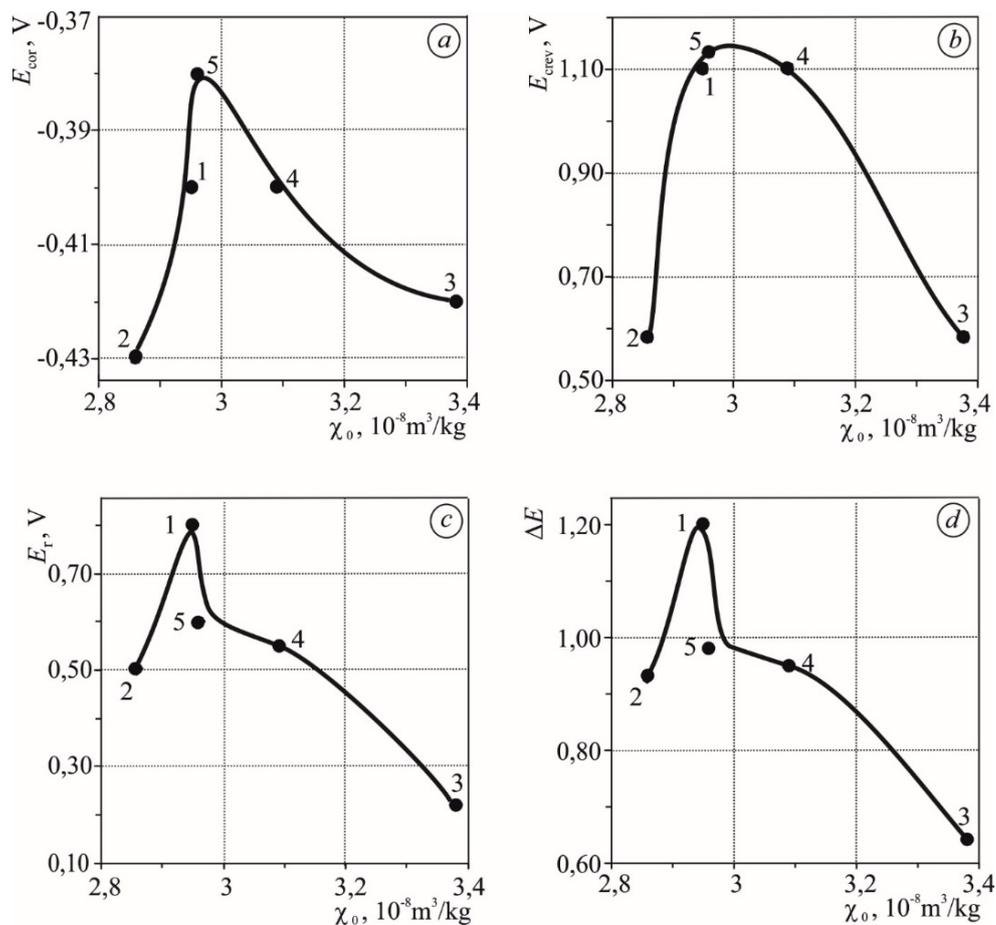
Figure 3 – Dependence of potentials E_{cor} (a), E_{crew} (b) and E_r (c) and crevice corrosion resistance basis ΔE (d) of 06KhN28MDT alloy on its specific magnetic susceptibility (χ_0)

The analysis (Fig. 3 b) showed that the E_{crew} potential of the 06KhN28MDT alloy rapidly shifts to the more positive side from 0.58 (melt 2) to 1.13 V (melt 5) with an increase in the parameter (χ_0) in it from $2.86 \cdot 10^{-8}$ (melt 2) to $2.96 \cdot 10^{-8}$ m³/kg (melt 5) (table 2). But then it intensively shifts to a more negative side from 1.10 (melt 4) to 0.58 V (melt 3) (Fig. 3b). It turns out that the maximum value of $3.38 \cdot 10^{-8}$ (melt 3) and the minimum value of $2.86 \cdot 10^{-8}$ m³/kg (melt 2) of the χ_0 parameter correspond to the most negative value of the E_{crew} potential (Fig. 3 b). In the melts 2, 3 alloy 06KhN28MDT with a maximum carbon content of 0.067 and 0.068 wt. %, respectively (Table 2), the same value of E_{crew} potential has been found (Fig. 2b). Most likely, this is due to precipitation of carbides from a supersaturated solid solution of austenite of the alloy, which affects its grain size (see Fig. 4).

It should be noted that the maximum value of the mean austenite grain diameter of 31 μm (Fig.

4) and one of the most positive values of the Ecrew potential of 1.10 V (Fig. 5b) correspond to the lowest carbon content in the alloy (0.048 wt.%, melt 4), and melts 2, 3 are the most negative (0.58V).

It has been established that in the melts 1, 5 with the smallest mean diameter of the austenite grain (11 and 15 μm), it is 1.10 and 1.13V, respectively (Fig. 5b).
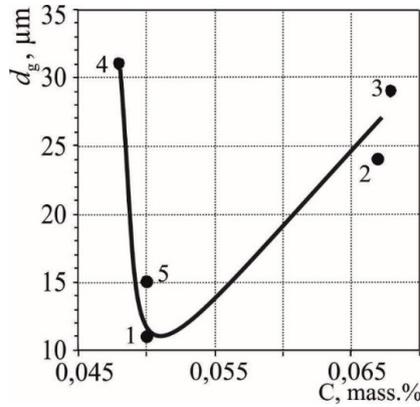

Figure 4 – Dependence of the mean austenite grain diameter (d) of the 06KhN28MDT alloy on its carbon content
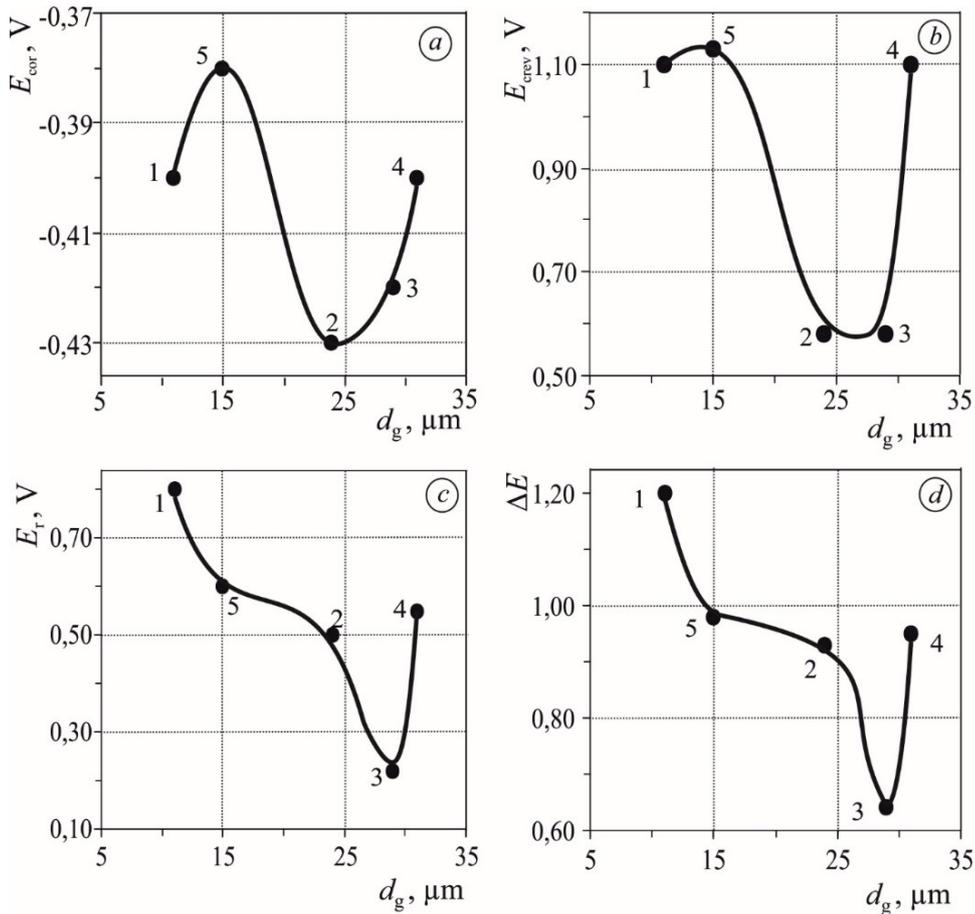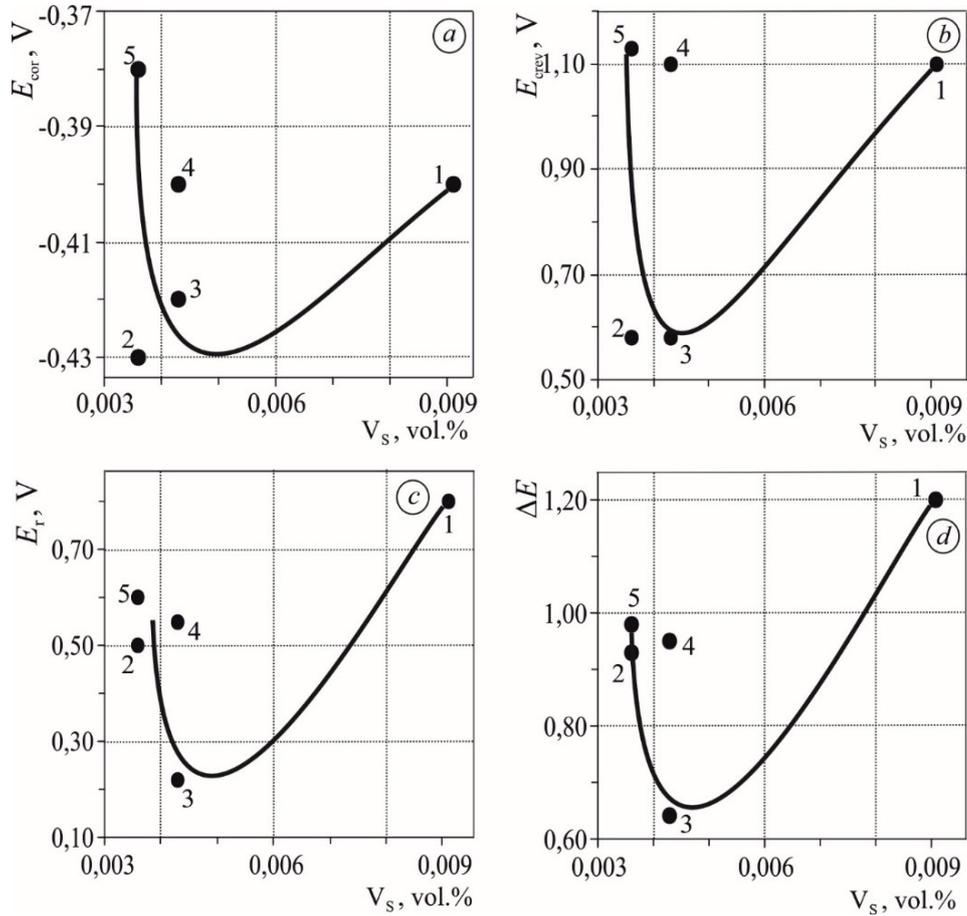

Figure 5 – Dependence of the potentials E_{cor} (a), E_{crew} (b) and E_r (c) and the crevice corrosion resistance basis ΔE (d) of the 06KhN28MDT alloy on the mean diameter of the austenite grain

According to the results of the analysis (Fig. 6a), it has been found that the melts 1, 4, 5 of the 06KhN28MDT alloy, which contain 0.0091, 0.0043 and 0.0036 vol. % of titanium sulfides (Fig. 7), have the most positive potential values of E_{crew} 1.10; 1.13 V, respectively.

**Figure 6** – Dependence of the potentials E_{cor} (a), E_{crew} (b) and E_r (c) and the crevice corrosion resistance basis ΔE (d) of the 06KhN28MDT alloy on the volume of titanium sulfides
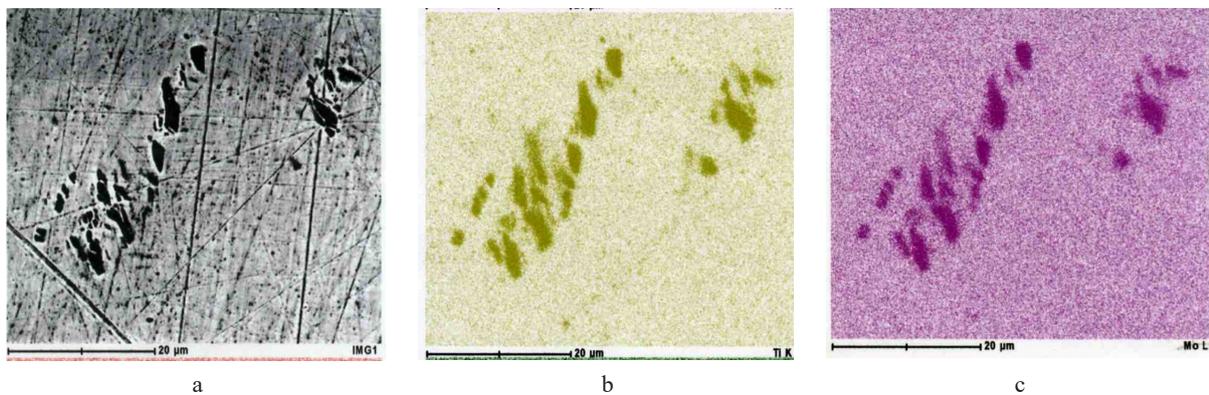
Figure 7 – Titanium sulfides in the 06KhN28MDT alloy (×1200)
a) metallography of titanium sulfides in the 06KhN28MDT alloy (x1200)
b) identification of titanium (energy dispersive topography)
c) identification of sulfur (energy dispersive topography)

At the same time, it should be noted that melts 2, 3 with the smallest volume of these inclusions in the alloy 0.0036 and 0.0043 vol. %, respectively, have the most negative value of the E_{crew} potential of 0.58 V and melts 4, 5 with the same volume of titanium sulfides – the most positive values are 1.10 and 1.13 V (Fig. 6, b). This shows that titanium sulfides (Fig. 6, b), the mean diameter of the austenite grain (Fig. 5, b), and the specific magnetic susceptibility of the alloy (Fig. 3, b) have a complex effect on its resistance to crevice corrosion in circulating water, since corrosion ulcers appear in the vicinity of these inclusions, mainly at the intersection with the boundaries of austenite grains. This is consistent with the data of papers [30-32] for AISI304 and AISI321 steels under similar research conditions. Their development depends on the properties of the austenite matrix, which is characterized by specific magnetic susceptibility, but the C content in the alloy clearly strongly affects this potential, because it intensively shifts to the more negative side with an increase in its C content (Fig. 2 b). It should be noted that the nature of the inclusions in the 06KhN28MDT alloy affects the E_{crew} potential, since there is no correlation between it and the volume of titanium carbonitrides (Fig. 8).
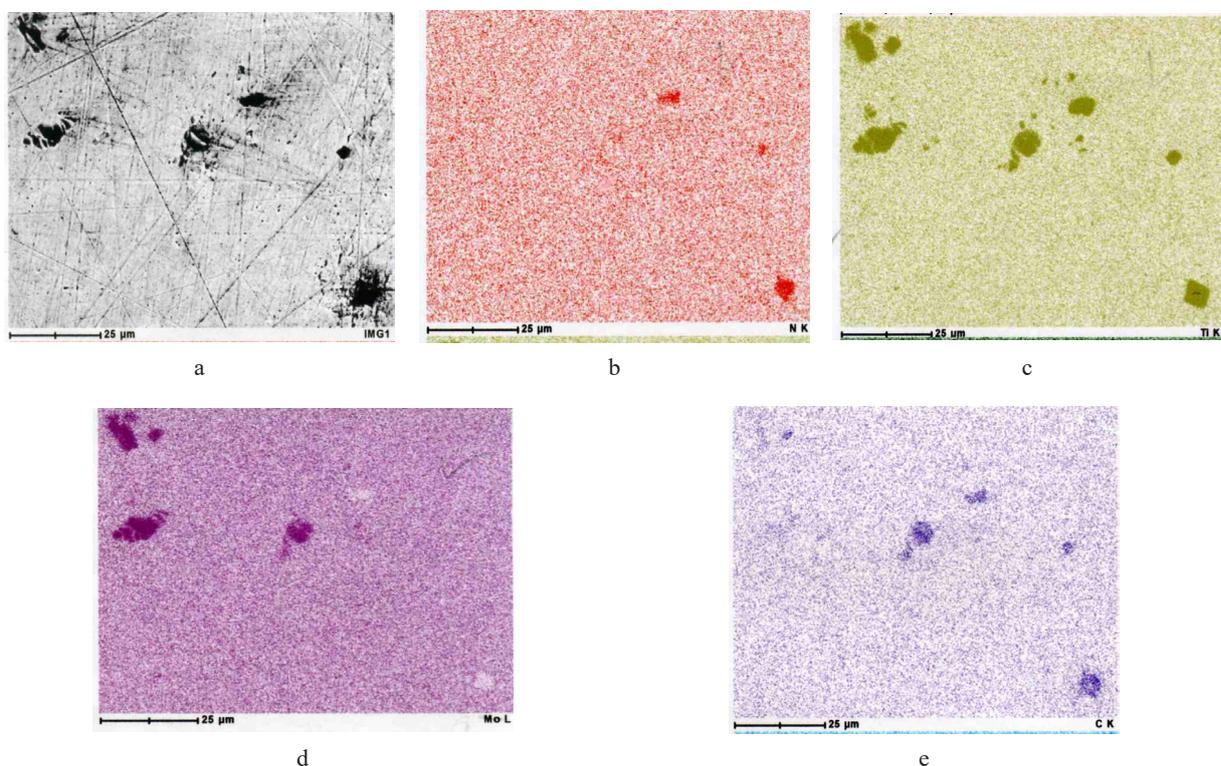
Figure 8 – Titanium nitride and accumulation of titanium sulfides in the 06KHN28MDT alloy (x550)
a) metallography of titanium sulfides in the 06KhN28MDT alloy (x1200)
b) identification of N (energy dispersive topography)
c) identification of Ti (energy dispersive topography)
d) identification of S (energy dispersive topography)
e) identification of C (energy dispersive topography)

It has been established that there is no correlation between the potentials of E_{cor}, E_{crew}, E_r, the ΔE criterion and the volume of titanium carbonitrides and sulfides, but melts 1, 5 correspond to the most positive values of the potentials, E_{cor}, E_{crew} and E_r (Fig. 6 a, b, c), and the smallest values of the mean diameter of the austenite grain (Fig. 5) and the highest total content of Cr, Mo and Cu (melts 5-6, 19 and melts 1-6, 41 wt.%) correspond to the largest basis of the resistance of the alloy to crevice corrosion ΔE (Fig. 9).
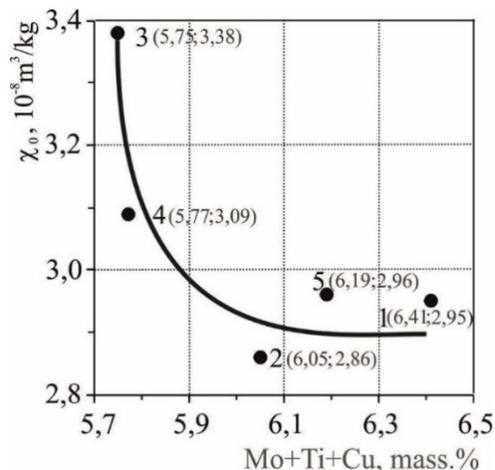
Figure 9 – Dependence of specific magnetic susceptibility χ_0 of austenite of the 06KHN28MDT alloy from the total content of molybdenum, titanium and copper

It should be noted that a similar trend for the dependences of E_{cor}, E_{crew}, E_r, ΔE (χ_0) has been established (Fig. 3), and the maximum total values of Mo, Ti and Cu (Fig. 9) and the minimum C (Table 1) correspond to the minimum values of the indicator $\chi_0 = 2.96 \cdot 10^{-8}$ and $2.95 \cdot 10^{-8}$ m³/kg melts 5 and 1, respectively (Table 2). At the same time, in the melt 3 of the alloy, the most negative value of the potentials Ecrew, Er and the smallest basis of its crevice corrosion resistance ΔE at the highest C content (0.068 wt. %) (Fig. 2 b, c, d), its χ_0 index (3.38·10⁻⁸ m³/kg) (Fig. 3 b, c, d) and the closest to the maximum value of the austenite grain (29 μm) (Table 2) and at the lowest – the total content of Mo, Ti and Cu (5.75 wt. %) have been observed (Fig. 9).

Melt 2 of the 06KhN28MDT alloy, like No. 3, has the lowest resistance to crevice corrosion in the model circulating water, since its potential Ecrew = 0.58V, and ΔE = 0.93V, which is less than that of melts 1, 4, 5 (Table 2). At the same time, melts 2 and 3 have the smallest (2.86·10⁻⁸ m³/kg) and the largest (3.38·10⁻⁸ m³/kg) values of the χ_0 indicator (Table 2). Most likely, this trend is due to the fact that in the melts 3 and 2 have a similar content of carbon (0.068 and 0.067 wt. %), chromium (21.82 and 22.69 wt. %) (Table 2), the total content of Mo, Ti and Cu (5.75 and 6.05 wt. %) (Fig. 9) and the size of the mean diameter of the austenite grain (29 and 24 μm) (Fig. 4), but they have the maximum melt 3 (3.38·10⁻⁸ m³/kg) and the minimum melt 2 (2.86·10⁻⁸ m³/kg) value of the χ0 indicator and the maximum (0.1918 vol. %) volume of titanium nitrides in melt 3 and close to the minimum – 0.1427 vol. % in melt 2 [10]. So, it turns out that slightly better resistance to crevice corrosion

melt 2, than No. 3 due to its higher content of chromium, the total content of molybdenum, titanium, copper and a much smaller volume of titanium nitrides and the value of the χ_0 parameter. Melts 1, 5 have the highest chromium content (24.29; 23.44 wt. %), the total content of Mo, Ti and Cu (6.41 and 6.19 wt. %), the minimum C content (0.050 wt. %) table. 2, close to the melt 2 values of the χ_0 indicator (2.95·10-8 and 2.96·10⁻⁸ m³/kg) and the most positive value of the Ecrew potential (1.10 and 1.13 V) and the largest ΔE (1.20 and 0.9V) (Table 2).

Taking into account the above and the data (Fig. 6), it can be noted that the main parameters of the 06KhN28MDT alloy that determine its resistance to crevice corrosion in circulating water are the content of Cr and C in it, the total content of Mo, Ti and Cu, and the volume of titanium sulfides. This is most likely due to the fact that Cr, Mo and Ti, forming mixed oxide films on the surface of the alloy, increase its resistance to crevice corrosion in circulating water. In addition, as is known [18], Mo and Cu increase the content of Cr in the oxide film, the protective properties of which are determined by the potentials of the Ecrew alloy in a chloride-containing media [15, 20] and the volume of titanium sulfides in it (Fig. 7) [10]. The specific magnetic susceptibility of the χ_0 alloy characterizes its atomic-magnetic state, which depends on the content, first of all, of the chemical elements Cr, Mo and Ti, which are paramagnetic [34].

4 Conclusions

According to the results of corrosion studies of the alloy 06KhN28MDT (similar to AISI904L steel) in model circulating water, it has been established that its potential Ecrew shifts in a more positive direction from 0.58 (melts 2, 3) to 1.10 and 1.13 V melts 1, 5 with an increase in its Cr content from 21.82 and 22.69 (melts 2, 3) to 24.29 and 23.44 wt.% (melts 1, 5), the total content of Mo, Ti and Cu from 6.05 and 5.75 melts 2, 3 to 6.41 and 6.19 wt. % melts 1, 5 and a decrease in the C content from 0.067 and 0.068 melts 2, 3 to 0.05 wt. % melts 1, 5. This helps to increase the resistance of the oxide film on the surface of the alloy to crevice corrosion due to the formation of mixed Cr, Mo, Ti oxide films enriched in Cr due to the activating effect of Cu. Reducing the content of C in the alloy to its solubility in the solid austenite solution prevents the precipitation of Cr, Ti, and Mo carbides in the vicinity of titanium nitrides, which has a positive effect on the resistance of the oxide film to "breakdown" by chlorides in the gap near these inclusions. These chemical elements also contribute

to the growth of the basis of the resistance of the alloy to crevice corrosion ΔE from 0.64 and 0.93 melts 3, 4 to 1.2 and 0.98 V melts 1, 5 with a change in their content in the mentioned interval has been established. This is due to the fact that the potential Er of the alloy shifts to a more positive side, and Ecor to a more negative side with an increase in the content of Cr, Mo, Ti, Cu and a decrease in C. It is shown that the specific magnetic susceptibility of the alloy χ0 is an integral characteristic that characterizes the atomic-magnetic state and depends on the content of these chemical elements. It is assumed that Ti sulfides can

determine the potentials of the alloy 06KhN28MDT Er, Ecor, Ecrew, affecting the protective properties of mixed Cr, Mo, Ti oxide films.

The melts 1.5 of the 06KhN28MDT alloy, which are the most resistant to crevice corrosion, experienced the greatest corrosion damage has been established. This is caused by the process of redistribution of current density between local corrosion damages due to repassivation of most metastable, due to the formation of mixed Cr, Mo, Ti oxide films, since these melts contain the largest amount of these alloying elements.

References

1. Kovalenko I.V. and Malinovsky V.V. Basic processes, machines and apparatus of chemical production: textbook. – Kyiv: Inres: Volia, 2015. – P. 264 (in Ukrainian)

2. Melik Çetin, Ali Günen, Müge Kalkandelen, Mustafa Serdar Karakaş. Microstructural, wear and corrosion characteristics of boronized AISI 904L superaustenitic stainless steel // Vacuum. – 2021. – Vol. 187 (5). – P. 110-145. https://doi.org/10.1016/j.vacuum.2021.110145

3. Narivs'kyi O. E. Micromechanism of corrosion fracture of the plates of heat exchangers // Materials Science. – 2017. – Vol. 43, no. 1. – P. 124–132. https://doi.org/10.1007/s11003-007-0014-3

4. Narivs'kyi O.E. Corrosion fracture of plate-like heat exchanger // Materials Science,– 2015. Vol. 1 (41). – P. 122-128. https://doi.org/10.1007/s11003-005-0140-8.

5. Zhanabaev, Z.Zh., Grevtseva, T.Yu., Gonchar, K.A., Mussabek G.K., Yermukhamed D., Serikbayev A., Assilbayeva R.B., Turmukhambetov, A.Zh., Timoshenko, V.Yu. Nonlinear analysis of the degree of order and chaos of morphology of porous silicon nanostructures // CEUR Workshop Proceedings. – 2019. – Vol. 2391. – P. 187-197. http://dx.doi.org/10.18287/1613-0073-2019-2391-187-197

6. Mussabek, G., Yermukhamed, D., Sarsembek, S., Almasuly, K., Sivakov, V. Electrochemical etching of p-type gallium phosphide // International Multidisciplinary Scienti c GeoConference Surveying Geology and Mining Ecology Management, SGEM. – 2018. – Vol. 18(6.1). – P. 185-190. https://doi.org/10.5593/sgem2018/6.1/S24.025

7. Markhabayeva A., Abdullin K., Kalkozova Zh., Nurbolat Sh., Nuraje N. Effect of synthesis method parameters on the photocatalytic activity of tungsten oxide nanoplates // AIP Advances. – 2021. – Vol. 11. – P. 095220. https://doi.org/10.1063/5.0065156

8. Narivskiy A., Yar-Mukhamedova G., Temirgaliyeva. E., Mukhtarova M. and Yar-Mukhamedov Y. Corrosion losses of alloy 06KhN28MDT in chloride-containing commercial waters // International Multidisciplinary Scientific GeoConference Surveying Geology and Mining Ecology Management: SGEM. – 2016. – Vol. 1. – P. 63–70.

9. Narivskiy A., Atchibayev R., Muradov A., Mukashev K. and Yar-Mukhamedov Y. Investigation of electrochemical properties in chloride-containing commercial waters // 18th International Multidisciplinary Scientific GeoConference SGEM2018. – [S. l.]. – 2018. – P. 267–274. DOI: 10.5593/sgem2018/6.1/S24.036

10. Narivs'kyi O. E. and Belykov S. B. Pitting resistance of 06KhN28MDT alloy in chloride-containing media // Materials Science. – 2018. – Vol. 44. – no. 4. – P. 573–580. https://doi.org/10.1007/s11003-009-9107-5

11. Narivskyi O.E., Subbotin S.A., Pulina T.V. and Khoma M.S. Assessment and Prediction of the Pitting Resistance of Plate-Like Heat Exchangers Made of AISI304 Steel and Operating in Circulating Waters // Materials Science. – 2022. – No. 58. – P. 41–46. https://doi.org/10.1007/s11003-022-00628-4

12. Narivskyi O.E., Belikov S.B., Subbotin S.A. and Pulina T.V. Influence of Chloride-Containing Media on the Pitting Resistance of AISI 321 Steel // Materials Science. – 2021. – Vol. 57, no. 2. – P. 291–297. DOI:https://doi.org/10.1007/s11003-021-00544-z

13. Narivs'kyi O., Atchibayev R., Kemelzhanova A., Yar-Mukhamedova G., Snizhnoi G., Subbotin S. and Beisebayeva A. Mathematical Modeling of the Corrosion Behavior of Austenitic Steels in Chloride-Containing Media During the Operation of Plate-Like Heat Exchangers // Eurasian Chemico-Technological Journal. – 2022. – Vol. 24, no. 4. DOI: https://doi.org/10.18321/ectj1473

14. Narivskyi O.E., Subbotin S.O., Pulina T.V., Leoshchenko S.O., Khoma M.S., Ratska N.B. Modeling of pitting of heat exchangers made of 18/10 type steel in circulating waters // Materials Science, 2023. Vol 58(5). P.1-7. https://doi.org/ 10.1007/s11003-023-00725-y

15. Ha H.-Y., Lee T.-H., Bae J.-H. and Chun D. W. Molybdenum Effects on Pitting Corrosion Resistance of FeCrMnMoNC Austenitic Stainless Steels // Metals. – 2018. – Vol. 8(8). – P. 653. https://doi.org/10.3390/met8080653

16. Fiorillo F. Measurement and Characterization of Magnetic Materials – Amsterdam: Elsevier. -2014. – P. 647.

17. Lakkam K., Kerur S.M. and Shirahatti A. Effect of pitting corrosion on the mechanical properties of 316 grade stainless steel// Materials today: Proceedings. – 2020. – No. 27 (1) – P. 497-502. https://doi.org/10.1016/j.matpr.2019.11.293

18. Yu Y., Shironita S., Souma K., Umeda M. Effect of chromium content on the corrosion resistance of ferritic stainless steels in sulfuric acid solution // Heliyon. – 2018. – Vol. 4 (11). – e00958. https://doi.org/10.1016/j.heliyon.2018.e00958

19.   Lynch B., Wang Z., Ma L., Paschalidou E.-M., Wiame F., Maurice V. and Marcus P. Passivation-Induced Cr and Mo Enrichments of 316L Stainless Steel Surfaces and Effects of Controlled Pre-Oxidation // Journal of The Electrochemical Society. – 2020. – Vol. 167. – 12p. https://doi.org/10.1149/1945-7111/abc727

20.   Silva P.M.O., Filho M.C.C., da Cruz J.A., Sales A.J.M., Sombra A.S.B. and Tavares J.M.R.S. Influence on Pitting Corrosion Resistance of AISI 301LN and 316L Stainless Steels Subjected to Cold-Induced Deformation // Metals. – 2023. – Vol. 13(3). – P. 443. https://doi.org/10.3390/met13030443

21.   Vignal V., Voltz C., Thiébaut S., Demésy M., Heintz O. and Guerraz S. Pitting Corrosion of Type 316L Stainless Steel Elaborated by the Selective Laser Melting Method: Influence of Microstructure // Journal of Materials Engineering and Performance. – 2021. – Vol. 30. – Pp. 5050-5058. https://doi.org/10.1007/s11665-021-05621-7

22.   de Lacerda J.C., Cândido L.C. and Godefroid L.B. Corrosion behavior of UNS S31803 steel with changes in the volume fraction of ferrite and the presence of chromium nitride // Materials Science & Engineering A. – 2015. – 648. – P. 428-435.

23.   Fuertes Nuria. Use of localised techniques to elucidate the in¬ uence of process variables on the corrosion of stainless steels // Doctoral Thesis in Chemistry. – KTH Royal Institute of Technology. – Stockholm, Sweden. – 2021. – P.115.

24.   Dalmau-Borrás A.; Richard C.; Igual Muñoz, A.N. Degradation mechanisms in martensitic stainless steels: wear, corrosion and tribocorrosion appraisal // Tribology International. – 2018. – Vol. 121. – P. 167 – 179. https://doi.org/10.1016/j.triboint.2018.01.036

25.   Szewczyk-Nykiel A. The influence of molibdenum on corrosion resistance of sintered austenitic stainless steels // Technical Transactions. – 2015. – Vol. 26. – P. 131-142. https://doi.org/10.4467/2353737XCT.15.344.4865.

26.   Yangting S., Xin T., Rulei L., Guoyong R., Jin L. and Yiming J. Mechanisms of inclusion-induced pitting of stainless steels: A review // Journal of Materials Science and Technology. – 2023. – Vol. 168. – P. 143-156. https://doi.org/10.1016/j.jmst.2023.06.008

27.   Diyuk, N.V., Keda, T.Y., Zaderko, A.N., Mussabek G.K., Nadtoka O. M., Kutsevol, N.V., Lisnyak, V.V. Luminescent carbon nanoparticles immobilized in polymer hydrogels for pH sensing // Applied Nanoscience. – 2022. – Vol. 12. – P. 2357-2365. https://doi.org/10.1007/s13204-022-02536-0

28.   Mussabek, G., Zhylkybayeva, N., Baktygerey, S., Taurbayev Y., Sadykov G. Zaderko, A.N., Lisnyak, V.V. Preparation and characterization of hybrid nanopowder based on nanosilicon decorated with carbon nanostructures // Applied Nanoscience. – 2023. – Vol. 13. – P. 6709-6718. http://dx.doi.org/10.1007/s13204-022-02681-6

29.   Sun Y.-T., Tan X., Lei L.-L., Li J. and Jiang Y.-M. Revisiting the effect of molybdenum on pitting resistance of stainless steels // Tungsten. – 2021. – Vol. 3. – P. 329-337. https://doi.org/10.1007/s42864-021-00099-1.

30.   Narivs'kyi O. E. Corrosion Fracture of Platelike Heat Exchangers // Fiz.-Khim. Mekh. Mater., 2015, 41 (1), pp, 104-108. https://doi.org/10.1007/s11003-005-0140-8.

31.   Narivs'kyi O.E. The influence of heterogeneity steel AISI321 on its pitting resistance in chloride – containing media // Materials Sciencem – 2017. – Vol. 2 (43). – P. 256-264. https://doi.org/10.1007/s11003-007-0029-9

32.   Mishchenko V. G., Snizhnoi G. V., and Narivs'kyy O. Eh. Magnetometric Investigations of Corrosion Behaviour of AISI 304 Steel in Chloride-Containing Environment // Metallofizika i noveishie technologii. – 2021. – Vol.33 (6). – P. 769-774. https://mfint.imp.kiev.ua/ru/toc/v33/i06.html. WOS:000296945600005

33.   Li P. and Du M. Effect of chloride ion content on pitting corrosion of dispersion-strengthened-high-strength steel // Corrosion Communications. – 2022. – Vol. 7. – P.23-34. https://doi.org/10.1016/j.corcom.2022.03.005

34.   de Rezendea S.C., Dainezia I., Apolinarioa R.C., de Sousaa L.L., Marianoa N.A. Influence of Molybdenum on Microstructure and Pitting Corrosion Behavior of SolutionTreated Duplex Stainless Steel in a Lithium Chloride Solution // Materials Research. – 2019. – Vol. 22 (1). – e20190138. http://dx.doi.org/10.1590/1980-5373-MR-2019-0138.